Published in final edited form as:
J Vis. ; 7(3): 5. doi:10.1167/7.3.5.

Glass pattern responses in macaque V2 neurons

Matthew A. Smith,
Center for Neural Science, New York University, New York, NY, USA, & Center for the Neural Basis of Cognition, Carnegie Mellon University, Pittsburgh, PA, USA

Adam Kohn, and
Center for Neural Science, New York University, New York, NY, USA, & Department of Neuroscience, Albert Einstein College of Medicine, Bronx, NY, USA

J. Anthony Movshon
Center for Neural Science, New York University, New York, NY, USA

Matthew A. Smith: mattsmith@cmu.edu; Adam Kohn: akohn@aecom.yu.edu; J. Anthony Movshon: movshon@nyu.edu

Abstract

Area V2 of macaque visual cortex is known to respond well to conventional oriented bar and grating stimuli, but some recent physiological data have shown that it may play an important role in coding more complicated patterns. Most of these data come from testing done with stimuli presented within the classical receptive field (CRF), whereas relatively little attention has been paid to the role played by the extraclassical surround. We have previously shown that neurons in primary visual cortex (V1) respond to translational Glass patterns in a manner that is predictable from their responses to grating stimuli. In this article, we first extend our experiments and modeling of Glass pattern responses in V1 to include V2. We explored the sensitivity of V2 cells to global form cues in Glass patterns confined to the CRF. Our results indicate that V2 neurons respond to the local signals in Glass patterns in a manner similar to V1 and that those responses are not influenced by global form present in the surround. It appears that the coding of the more complicated global structure in Glass patterns takes place further downstream in the visual system.

Keywords

form processing; contextual modulation; surround suppression; primary visual cortex; V1; extrastriate; random dots; Glass patterns; macaque monkey

Introduction

In the first stage of visual processing in primates, visual space is parsed into discrete regions by the neural circuitry of the retina. One of the tasks of our visual cortex is to combine the responses of individual neurons with spatially discrete receptive fields to produce a coherent picture of our environment. This pooling of local cues over space can be performed by mechanisms that act within and outside the classical receptive field (CRF) of a neuron. Physiological data exist in support of both of these methods of integration—(1) macaque extrastriate visual areas V2 (Hegdé & Van Essen, 2000, 2003, 2004; Peterhans & von der

Corresponding author: Matthew A. Smith., mattsmith@cmu.edu., Address: Center for the Neural Basis of Cognition, Carnegie Mellon University, 4400 Fifth Avenue, Mellon, Institute Room 115, Pittsburgh, PA 15213, USA.

Commercial relationships: none.

Heydt, 1993) and V4 (Gallant, Braun, & Van Essen, 1993, Gallant, Connor, Rakshit, Lewis, & Van Essen, 1996; Pasupathy & Connor, 1999, 2001, 2002) contain neurons sensitive to complex form information in stimuli confined to the CRF, and (2) contextual effects from outside the CRF are commonly observed in both striate (Blakemore & Tobin, 1972; DeAngelis, Freeman, & Ohzawa, 1994; Hubel & Wiesel, 1968; Knierim & Van Essen, 1992; Lamme, 1995; Nelson & Frost, 1978; Zipser, Lamme, & Schiller, 1996) and extrastriate (Allman, Miezin, & McGuinness, 1985; Born, 2000; Bradley & Andersen, 1998; Schein & Desimone, 1990; Solomon, Peirce, & Lennie, 2004; Thomas, Cumming, & Parker, 2002) visual cortex. Because these contextual effects may involve feedback or lateral cortical connections, they may only be present later in a response epoch. Several studies have found dynamics that are consistent with this view (Hegdé & Van Essen, 2004; Knierim & Van Essen, 1992; Lamme, 1995; Lee, Yang, Romero, & Mumford, 2002).

V2 receptive fields are larger than those in V1 and show evidence of integration of simple features to link to more complex percepts (Hegdé & Van Essen, 2000, 2003, 2004). This makes V2 an excellent area in which to study the relative importance of CRF and surround effects in form vision and the integration of local features to form global percepts. A variety of approaches and stimuli make it difficult to compare results across studies and visual areas. Nevertheless, a growing body of evidence suggests that neurons in area V2 differ from those in V1 in their responses to form and contextual stimuli, although they respond similarly to conventional gratings (Levitt, Kiper, & Movshon, 1994) and exhibit comparable iso-orientation surround suppression (Solomon et al., 2004). Some V2 neurons respond to illusory contours when the actual stimulation is outside their CRF (Lee & Nguyen, 2001; Peterhans & von der Heydt, 1989; von der Heydt, Peterhans, & Baumgartner, 1984), show evidence of border ownership coding (Zhou, Friedman, & von der Heydt, 2000), prefer non-Cartesian gratings (Mahon & DeValois, 2001), and are sensitive to shape-from-shading stimuli (Lee et al., 2002). These extraclassical influences may play a significant role in texture segmentation and contour detection (Nothdurft, Gallant, & Van Essen, 1999, 2000; Petkov & Westenberg, 2003). It appears that V2 is a good candidate area for the study of the early stages of form vision.

One difficulty in the systematic study of form vision has been choosing a suitable stimulus to use in characterizing neural responses. Most research has focused on object primitives such as curved edges, junctions, and elementary shapes (Brincat & Connor, 2004; Gallant et al., 1993, 1996; Hegdé & Van Essen, 2000, [2003], [2004]; Pasupathy & Connor, 1999, 2001, 2002; Peterhans & von der Heydt, 1993). Glass patterns (Glass, 1969; Glass & Perez, 1973) are texture stimuli made by pairing a “seed” pattern of randomly placed dots with a set of partner dots shifted according to a particular geometric rule (see Figure 5 for examples). These patterns evoke a strong percept of global form, which arises only from sparse local orientation cues. Two features of Glass patterns make them ideal for studying form vision, inspiring their use in numerous psychophysical studies in human observers (Cardinal & Kiper, 2003; Dakin, 1997; Dakin & Bex, 2001; DeValois & Switkes, 1980; Earle, 1985; Glass & Switkes, 1976; Mandelli & Kiper, 2005; Prazdny, 1984, 1986; Ross, Badcock, & Hayes, 2000; Wilson & Wilkinson, 1998; Wilson, Wilkinson, & Asaad, 1997). First, through varying parameters of the dot pattern, it is possible to perform quantitative manipulations of the form percept. This makes them an appealing compromise between highly complex but poorly parameterized stimuli, like natural scenes, and simple but artificial stimuli, like bars or gratings. Second, consideration of the structure of Glass patterns indicates that they are processed in two stages. The first stage identifies weak local orientation cues in the pattern, and the second stage integrates these local signals to extract global form information.

In our previous study of primary visual cortex (Smith, Bair, & Movshon, 2002), we reasoned from models and confirmed with data that the tuning of V1 cells to Glass patterns could largely be explained by understanding a neuron's response to a translational Glass pattern confined to the CRF. However, V1 neurons did not appear to provide strong signals about global Glass pattern structure based on information present outside their receptive fields. This led us to believe that the second stage of extracting and pooling global form information takes place outside of V1. Several models have proposed a multistage processing of Glass patterns, which is consistent with this idea (Barlow & Olshausen, 2004; Wilson & Wilkinson, 1998; Wilson et al., 1997). In this study, we turned our attention to considering the role of V2 in Glass pattern perception. We first compare the responses of individual neurons in V1 and V2 of macaque monkeys to Glass pattern stimuli. We show that for translational patterns, V2 neurons have tuning for dot-pair orientation and separation that is consistent with what we observe in V1 neurons. We also use concentric and radial Glass patterns to probe the responses of V2 cells to global form information presented outside of their CRF. Our results show no significant sensitivity of V2 neurons to concentric or radial Glass pattern form presented outside their CRF. We conclude that V2 plays a role similar to V1 in processing the sparse form cues present in Glass pattern stimuli.

The findings presented in this article have appeared previously in abstract form (Movshon, Smith, & Kohn, 2003).

Methods

Electrophysiology

We recorded extracellularly from single units in V1 and V2 of two cynomolgus macaques (*Macaca fascicularis*) and three bonnet macaques (*M. radiata*), whose weight ranges from 3.1 to 4.6 kg.

The techniques used in our laboratory for recording from the visual cortex of anesthetized, paralyzed primates have been reported in detail elsewhere (Cavanaugh, Bair, & Movshon, 2002a). Briefly, animals were premedicated with atropine sulfate (0.05 mg/kg) and diazepam (Valium, 1.5 mg/kg) 30 min prior to inducing anesthesia with ketamine HCl (10.0 mg/kg). We continued anesthesia on 1–2% isoflurane in a 98% O_2/2% CO_2 mixture during the initial surgery. We inserted catheters into the saphenous veins of the hindlimbs and performed a tracheotomy. We mounted the animal in a stereotaxic apparatus, made a craniotomy and durotomy over the opercular portion of V1, and then discontinued gas anesthesia. Anesthesia was maintained throughout the rest of the experiment by a continuous infusion of sufentanil citrate (typically 4 μg/kg, established for each animal) mixed with a lactated ringer's solution (Normosol). Infusion solutions were mixed to 2.5% dextrose concentration to provide adequate nutrition, and infusion rate was adjusted to maintain fluid balance (approximately 4–8 $ml \cdot kg^{-1} \cdot hr^{-1}$). Vital signs (EEG, ECG, end-tidal pCO_2, temperature, and lung pressure) were monitored continuously. Expired pCO_2 was maintained between 3.9% and 4.7% (30–36 mm Hg). Rectal temperature was maintained near 37°C through the use of a heating pad. To minimize eye movements, we paralyzed the animal with a continuous intravenous infusion of vecuronium bromide (Norcuron, 0.1 $mg \cdot kg^{-1} \cdot hr^{-1}$). The pupils were dilated with topical atropine, and the corneas were protected with gas-permeable, hard contact lenses. We used supplementary lenses to bring the retinal image into focus by direct ophthalmoscopy. We later adjusted the refraction further to optimize the response of recorded units. We gave daily injections of a broad-spectrum antibiotic (Bicillin) and an anti-inflammatory agent (dexamethasone). Experiments typically lasted 4–5 days. All procedures complied with guidelines approved by the New York University Animal Welfare Committee.

We recorded with quartz–platinum–tungsten microelectrodes (Thomas Recording, Giessen, Germany), advanced with a mechanical microdrive system through a small durotomy made within a craniotomy of approximately 10 mm in diameter. The craniotomy was typically centered 4 mm posterior to the lunate sulcus and 10 mm lateral to the midline. For V2 recordings, the electrode was typically advanced down in the parasagittal plane, angled slightly away from vertical (roughly 30°) in the anterior direction. With this configuration, receptive field eccentricities of V2 neurons are typically from 2° to 6°. We recorded V1 neurons on the operculum and in the calcarine sulcus, where the receptive field eccentricities are typically 2–5° and 8–25° of visual angle, respectively. Signals from the microelectrode were amplified and bandpass filtered, and we isolated single units with a dual-window time–amplitude discriminator (Bak, Germantown, MD). The time of each action potential was recorded with a resolution of 0.25 ms by a CED-1401 Plus laboratory interface (Cambridge Electronic Design, Cambridge, UK).

Visual stimulus generation

We displayed all visual stimuli at a resolution of 1,024 × 731 pixels and a video frame rate of 100 Hz on either a Nanao T550i or Eizo T550 monitor. We used lookup tables to correct for nonlinearities in the relation between input voltage and phosphor luminance in the monitors. We generated drifting sinusoidal grating stimuli with a Cambridge Research Systems VSG 2/2 board (Kent, UK) running on an Intel x86-based host computer and random dot stimuli with a Silicon Graphics workstation. The mean luminance of the display was approximately 33 cd/m^2 when displaying gratings. All of the gratings were presented at 100% contrast in a circular aperture surrounded by a gray field of the average luminance.

For each isolated neuron, we began by mapping its receptive field for each eye on a tangent screen by hand. We determined the dominant eye to be that which yielded the larger response and occluded the other eye. Using a front surface mirror, we brought the receptive field into register with the center of the video monitor placed 135 cm from the animal's eye, where it subtended 13° of visual angle. We then proceeded with experiments under computer control.

We characterized the cell's response properties to gratings in this order: (1) orientation and direction tuning, (2) spatial frequency tuning, (3) temporal frequency tuning, and (4) size tuning. We chose a small patch of optimized grating and adjusted the vertical and horizontal position by hand to obtain the maximal response. This patch was taken to be centered in the receptive field. These experiments consisted of multiple blocks of stimuli, each composed of a randomly ordered group of all the stimuli in a set. All stimuli within a block were equal in duration and were separated by presentation of a uniform mean gray background for about 1.5 s. We classified cells as simple or complex using the standard F1:DC ratio (Movshon, Thompson, & Tolhurst, 1978; Skottun et al., 1991), where DC is the mean firing rate (minus baseline) and F1 is the amplitude of the Fourier component at the fundamental frequency of the response to an optimized drifting grating. Units were classified as simple if the F1:DC ratio of the preferred stimulus in their spatial frequency tuning curves was greater than 1; all other units were classified as complex.

Glass pattern characterization

Glass pattern stimuli consisted of randomly positioned dot pairs in which dot separation and pair orientation were constant across all pairs on a given trial. On each video frame (every 10 ms), a new set of dot pairs was plotted, which was independent of the previous frame. Thus, these patterns had local spatial structure within frames but no coherent spatial structure or motion between frames. We used these dynamic patterns to randomize the positions of the dots in the pattern over time and to minimize retinal adaptation at particular

dot positions. All dot patterns were presented within a circular aperture. Dots were presented at maximum contrast (i.e., white dots on a black background). The maximum luminance was 68.4 cd/m^2, and the minimum was near 0.0 cd/m^2. The mean luminance of the display was approximately 0.2 cd/m^2 while displaying white dots on a black background. Dot size was typically 0.04° (range, 0.03–0.12°), and density was typically 200 dots·deg^{-2}·s^{-1} (range, 100–800). In this range, human observers readily perceive Glass patterns, and variations in dot density have no significant impact on perception (Alliston, Friehling, Smith, Landy, & Movshon, 2001).

Glass pattern stimuli were presented in an extended sequence of 320-ms epochs with no screen blanks between them. Each epoch contained a different pattern of dots—no random sequence was ever repeated for a given neuron. Trials usually lasted 15 s, and stimuli were repeated five times in each trial. This entire sequence was then repeated to collect many repeats of each stimulus (typically 100) in a short period. This avoided any contamination with a luminance response because dot patterns with the same mean luminance on each video frame were presented throughout the duration of the stimulus. We determined the spontaneous response from 500 ms of blank screen preceding the stimulus. We found no significant differences between the V1 data collected using this method of stimulus presentation and our previous results (Smith et al., 2002), which were collected using a standard blocked experimental design (all stimuli were of equal duration, separated by a blank screen for about 1.5 s).

In our previous experiments in V1 (Smith et al., 2002), we used a dot field of the same size as the CRF, determined with grating stimuli. Because we found no significant alteration of tuning properties with field size, we used larger field sizes in these experiments. For each cell, we determined the CRF size from a size tuning curve taken with gratings. If the cell's responses showed surround suppression for large grating stimuli, we used a dot field that was the same size as the CRF. For cells that did not show significant surround suppression, we used a large dot field of approximately 6–8° in diameter.

For each neuron, we presented Glass patterns at eight orientations (θ) and five dot separations (*r*). The orientations were evenly spaced over 180° (Movie 1). On the basis of our previous results (Smith et al., 2002), we chose the range of *r* to include values from approximately λ/4 to 3λ/2, where λ was the preferred spatial period of the cell. For cells whose optimal *r* was at the top or bottom of our tested range, we collected additional data in a range that included the best *r* and both smaller and larger values. In all further Glass pattern experiments, we used the values of *r* and θ determined to optimize the cell's response modulation. If the preferred θ was unclear, we chose it to be aligned to the cell's optimal response to gratings.

Quantitative measures

The techniques we used to analyze our grating and Glass pattern data have been reported in detail previously (Smith et al., 2002). Briefly, for gratings and Glass patterns, data from size tuning curves were fit with the integral of a difference of Gaussians (DeAngelis et al., 1994). We chose the size of the CRF to be the smallest diameter stimulus for which the fitted curve reached 95% of its maximum. We also fit descriptive functions to spatial frequency tuning curves for gratings to find the optimal spatial period, λ (the inverse of the optimal spatial frequency), for each cell (Levitt et al., 1994).

To characterize orientation tuning curves, we determined the selectivity and preferred angle by calculating a tuning bias vector (Leventhal, Thompson, Lui, Zhou, & Ault, 1995; O'Keefe & Movshon, 1998; Smith et al., 2002). The selectivity index is 0 for a cell responding equally at all orientations and 1 for a cell that responds only to a single

orientation. To estimate the significance of each selectivity estimate, we performed the selectivity index analysis on 2,000 random permutations of the data in each tuning curve and considered a measured selectivity index to be significant if it exceeded the 90th percentile of the permuted distribution. To estimate analogous quantities for tuning curves with four lobes (rather than two), which we term “quadropoles,” we modified the tuning bias equations. This resulted in a measure of preference and bias appropriate for functions with periodic peaks and troughs every 90°, rather than every 180°.

Results

We made extracellular recordings from 90 neurons (75 complex, 15 simple) in V2 and 33 neurons (21 complex, 12 simple) in V1 of five macaque monkeys. We characterized each cell with drifting sine wave gratings before testing with dynamic, translational Glass patterns. To increase the efficiency of our data collection and gather a large number of trials in a shorter period, we used a continuous sequence of 320-ms stimulus epochs, with no blank screen between presentations, to achieve a total of 100–200 repeats of each stimulus (Movie 1). This continuous stimulation method was different from the one used in our previous experiments in V1 (Smith et al., 2002), and for this reason, we recorded from both V2 and V1 neurons. This allowed us to make a direct comparison between V1 and V2 neuronal responses to an identical stimulus. The dot density was the same on each video frame to avoid any response to a change in luminance as each stimulus began. From the resulting spike trains, we parsed out the spike times corresponding to the response for each of the stimulus and determined the response rate from these data.

Glass pattern tuning within the CRF

In our previous study of V1 neurons (Smith et al., 2002), we found that tuning to translational Glass patterns was well matched to predictions of a linear model based on a Gabor filter receptive field. The preferred translational Glass pattern (defined as the one that produced the greatest response and selectivity for a given cell) tended to have a dot-pair orientation that matched that of the preferred grating and dot separation between one quarter and one half of the spatial period (λ) of the optimal grating. This is because at that separation, dot pairs tend to cancel (fall in opposite-polarity Gabor subfields) when aligned perpendicular to the RF orientation and reinforce (fall in the same-polarity Gabor subfield) when aligned parallel to the RF orientation. This dot separation therefore produces the largest changes in response with dot-pair orientation and the most robust tuning. We wanted to see if this linear model would also hold in V2 neurons for translational Glass pattern stimuli presented within their CRFs or if the results would differ from our findings in V1.

Using the stimulus method described above, we collected orientation tuning curves for translational Glass patterns at multiple dot separations (r) and dot-pair orientations (θ) and compared them to the tuning for drifting sinusoidal gratings in both V1 and V2. The tuning curves collected for two sample V2 neurons are shown in Figure 1. The orientation tuning of both cells to Glass patterns is quite strong (red solid lines) and well aligned with that to gratings (blue dotted line). Robust tuning appears over a range of dot separations between one quarter and one half of λ. Four-lobed tuning is weak but visible at higher values of r/λ, particularly in the cell in Figure 1A.

From the multiple Glass pattern tuning curves, we found the value of r for which the orientation tuning had the highest selectivity index (see the Methods section). Figures 2A and 2B show frequency histograms of the values of r/λ, which produced the highest orientation selectivity index in both V1 and V2, respectively. Although the mean of the V1 distribution (0.34 ± 0.20) was slightly lower than that of the V2 distribution (0.41 ± 0.43), the difference was not statistically significant (ANOVA, p = .37). In addition to the similar

mean value, the overall distribution of the optimal r and λ spanned a similar range and was significantly correlated in both our V1 (Pearson's $r = .36$, $p = .039$) and V2 ($r = .44$, $p < .0001$) cell populations. Using data with the dot separation that provided the best selectivity index, we estimated the preferred dot-pair orientation from the tuning curve using the vector strength calculation (see the Methods section). We compared the preferred orientation for a translational Glass pattern with that for gratings and plotted the resulting frequency histograms for V1 and V2 (Figures 2C and 2D). In both cortical areas, roughly 80% of the cells preferred a translational Glass pattern orientation in which the dot pair was aligned within 22.5° of the preferred grating orientation. As shown in Table 1, the average selectivity index in V1 (0.54 ± 0.12) and V2 (0.56 ± 0.15) was not significantly different (Wilcoxon test, $p = .23$). From these data, we conclude that the linear model provides a good means of predicting the preferences of V2 neurons to translational Glass patterns, similar to our previous findings in V1.

While the tuning for Glass patterns in both V1 and V2 is well captured by a linear model, the two areas may play a different role in the perception of Glass patterns due to a difference in responsivity. For this reason, we set out to compare this property quantitatively between V1 and V2 neurons. We calculated the response modulation for Glass patterns and gratings as the maximum minus the minimum response (peak − trough) of the orientation tuning curve. V2 cells responded less vigorously, on average, to both gratings and Glass patterns than did V1 cells. The mean values for response modulation for simple and complex cells in both V1 and V2 are shown in Table 2. The modulation in grating responses was significantly higher in V1 neurons than in V2 neurons for both simple cells (ANOVA, $p = .0001$) and complex cells ($p = .001$). The modulation in firing rate to Glass patterns showed a similar trend (V1 being higher than V2), although the differences were not statistically significant (simple cells, $p = .25$; complex cells, $p = .56$). The response ratio of gratings to Glass patterns was higher in V1 than in V2 for both simple and complex cells, although that difference was only significant for simple cells ($p = .03$). Figures 3A and 3B plot the modulation of response to Glass patterns for neurons in V1 and V2 against the response evoked by an optimal sinusoidal grating. In both areas, all points fell below the identity line, indicating that the neurons responded more vigorously to gratings than to Glass patterns. The geometric mean of the response ratio for Glass patterns was higher in V1 (8.0) than in V2 (4.9) across simple and complex cells, and this difference was statistically significant (ANOVA, $p = .005$). It appears from this analysis that there is a general trend for higher response modulation in V1 to both Glass patterns and gratings, as well as a larger ratio of Glass pattern to grating response.

Collectively, the data presented in this section indicate that V1 and V2 neurons show broadly similar selectivity to Glass pattern stimuli, although there are some significant differences in response strength. In both V1 and V2, the responses can be largely predicted by a linear model. However, previous work has identified complex form selectivity in the CRF of V2 neurons using other stimuli (Hegdé & Van Essen, 2000, 2003, 2004). Thus, it remains possible that V2 neurons might respond selectively to more complicated Glass pattern structure presented within the CRF.

Glass pattern tuning from beyond the CRF

Previous studies in macaque V2 with complex form stimuli have primarily confined them to the CRF. We have seen that for translational Glass pattern stimuli limited to the CRF, the responses of V1 and V2 neurons are remarkably similar. It is possible that V2 neurons play a role in Glass pattern processing through contextual mechanisms that are activated by stimuli extending beyond the CRF. We therefore wondered whether the form information present in an extended Glass pattern stimulus would be able to modulate the response of V2 neurons when the pattern presented in the CRF was the same. Consistent with integration on this

spatial scale, psychophysical experiments with Glass patterns have used fields that are typically 10° or more in diameter, positioned at the center of gaze, which extend well beyond the CRF of an individual V2 cell.

There have been many studies of suppression by stimuli outside the CRF in V1 cells (Blakemore & Tobin, 1972; Cavanaugh et al., 2002a; Cavanaugh, Bair, & Movshon, 2002b; DeAngelis et al., 1994; Hubel & Wiesel, 1968; Knierim & Van Essen, 1992; Nelson & Frost, 1978; Sceniak, Ringach, Hawken, & Shapley, 1999). However, although the responses of V1 and V2 neurons to gratings confined to the CRF have been reported to be similar in their orientation selectivity and spatial and temporal tuning (Levitt et al., 1994), we are aware of only one quantitative study of iso-orientation surround suppression in macaque V2 (Solomon et al., 2004). We set out to first provide an account of surround suppression effects in our population of V2 neurons, using grating stimuli and analysis methods identical to work previously performed in our laboratory (Cavanaugh et al., 2002a). After recording responses to gratings of increasing size, we fit each size tuning curve with the integral of a difference of Gaussians (DeAngelis et al., 1994; see the Methods section). The distribution of optimal sizes for our V1 and V2 neurons is shown in Figures 4A and 4C. V2 neurons averaged 1.57° in diameter, substantially larger than V1 neurons (0.92°) in a similar range of eccentricities. These values are consistent with those reported by Cavanaugh et al. (2002a) and Solomon et al. (2004) for V1 and V2, respectively. Thus, based on our data, it appears that the diameter of V2 receptive fields is roughly 1.5 times greater than V1.

To quantify the magnitude of suppression, we computed a suppression index (SI). This was defined as the peak response minus the response at the maximum size, divided by the response at the maximum size. The SI ranges from 0 (for no suppression) to 1 (for complete suppression). On average, neurons in V2 were suppressed by 38% of their maximum response by grating stimuli that extended beyond the CRF. Figures 4C and 4D show the distribution of SI for our population of V1 and V2 neurons, respectively. The mean SI for gratings was slightly higher in V2 than in V1 (0.38 ± 0.32 vs. 0.30 ± 0.25), but this difference was not statistically significant (ANOVA, $p = .22$) and the V1 sample was small ($n = 33$). A more comprehensive study found a mean SI of 0.38 in V1 (Cavanaugh et al., 2002a), which is the same value we found for our V2 population.

We have observed that V2 neurons demonstrate iso-orientation surround suppression similar to V1 neurons, but we also wanted to determine whether they exhibit more global integration for Glass pattern stimuli. Therefore, we developed stimuli that had the same characteristics in the CRF but had a different global form present on a larger scale. After finding the optimal r and θ for a translational Glass pattern, we presented a stimulus that filled the entire video display (12.9° × 9.3°). We used translational (Figure 5A), concentric (Figure 5B), and radial (Figure 5C) Glass patterns, as well as random dots, to test each cell. Translational Glass patterns were shown at the optimal r in either a preferred or orthogonal orientation. Concentric and radial Glass patterns were centered in one of four positions designed to stimulate the CRF with an approximation of an optimal translational Glass pattern while stimulating areas beyond the CRF with different global forms. From the center of each cell's receptive field, we found two positions (usually separated by one and two widths of the cell's receptive field) on either side of the center. The concentric and radial Glass patterns were centered at these distances on a line orthogonal (for concentric) or parallel (for radial) to the cell's preferred orientation (see Figures 5E–H for examples). If V2 neurons are sensitive to the presence of global form information outside the CRF, they should have different responses to the concentric or radial stimuli depending on their position.

We recorded from 20 neurons in V2 using this stimulus (Movie 2). These neurons were not selected for study based on their response properties to gratings or Glass patterns. Figure 6A shows the population response to each of the 11 stimuli. The response of each neuron to each stimulus type was normalized by the response to the preferred translational pattern (which was defined to be 100%). The lowest firing rate was for the same translational pattern in the orthogonal orientation (54%). The four concentric and four radial patterns showed responses that were similar to but slightly less than the preferred translational pattern (an average of 93%). The random pattern generated an intermediate response (60%). Although there was some variation among the responses to these eight stimuli, it was not statistically significant (ANOVA, $p = .06$). Individual neurons might have significant tuning that was not evident in the average across all neurons. We therefore used a bootstrap method to assess the statistical significance of tuning for each neuron. We tested whether the response to any of the eight global form stimuli deviated significantly from the mean response to all of the stimuli for each of the recorded neurons. There were no responses to any of the eight stimuli for any of the 20 neurons that showed a significant deviation from the mean (using a criterion of $p < .05$).

Although our measures of tuning did not show a systematic tuning for Glass pattern form in single neurons or the population, in some neurons, there appeared to be a greater response to the far concentric and radial stimuli than the near stimuli. We might expect such a difference even if V2 neuronal responses to these Glass pattern stimuli are primarily determined by the CRF. For both the concentric and radial patterns, there was greater variation in the dot-pair orientations in the receptive field for near stimuli than for far stimuli (compare the dots that fall in the CRF in Figures 5E and 5F). Thus, based on a linear Gabor filter model of the receptive field, we expect the response to the far stimuli to exceed that to the near stimuli. Alternatively, if iso-orientation surround suppression mechanisms were activated strongly by the concentric or radial patterns, the presence of more extended linear contours in the far stimuli would lead to more suppression. We found that the average response to all of the far stimuli (94.5%) was greater than that to the near stimuli (91.5%), and this difference was statistically significant ($p = .02$, uncorrected for multiple comparisons). This is qualitatively consistent with predictions from a linear model of the CRF uninfluenced by mechanisms outside the CRF. Furthermore, if iso-orientation surround suppression played a large role in the tuning for these stimuli, we would expect a decreased response to the translational pattern relative to concentric and radial. We observed just the opposite—the average response to concentric and radial patterns was 7% less than that to translational pattern ($p = .0002$). These same neurons had a reduced response for the full-screen translational patterns used here compared with the smaller patterns chosen for the CRF experiments. This indicates that although surround suppression mechanisms were activated by the Glass patterns, the selectivity of the cells' responses was determined by the stimulus presented to the CRF. Using this stimulus configuration, we found no evidence for significant tuning for the shape or position of global form in Glass pattern stimuli among our population of V2 neurons.

We did not observe significant Glass pattern tuning in the mean response, but we wondered whether a difference might be present in some small time window. Previous studies have shown that neurons may signal the presence of a global form or contextual modulation in the later parts of their response (Hegdé & Van Essen, 2004; Knierim & Van Essen, 1992; Lee et al., 2002; Zipser et al., 1996). We therefore compared a grand average response histogram for the different Glass patterns for all cells. Figure 6B shows the average firing rate across cells over time. From the stimulus onset to approximately 65 ms, the responses are overlapping. The average response during this period is approximately 14 ips and represents the mean firing evoked by all of the 11 stimuli. Thereafter, the response to a preferred translational pattern was consistently higher than the other responses (thick gray line). We

found that the responses to the concentric and radial patterns remained consistently lower than those to the preferred translational pattern. We averaged the two near and two far concentric patterns (*dashed black* and *solid black lines*) and four radial patterns (*dashed gray line*) for clarity of presentation. We therefore found nothing in the response time courses to challenge our conclusion from analysis of mean response.

Discussion

One obstacle to the electrophysiological study of form vision has been the difficulty of choosing a stimulus that proves effective in eliciting responses from higher cortical areas and can be varied quantitatively. The combination of these two properties appears necessary in determining the basis of receptive field structure in these cortical areas. Some attempts have involved the use of concentric or radial grating stimuli (Gallant et al., 1993, 1996; Hegdé & Van Essen, 2000, 2003, 2004), whereas others have used a set of object "primitives," consisting of corners and junctions (Brincat & Connor, 2004; Kobatake & Tanaka, 1994; Pasupathy & Connor, 1999, 2001, 2002). V2 has received attention as an area that might play an important role in form vision with its strong inputs from V1 and projections to V4 and other ventral visual areas. Neurons in V2 are known to respond to illusory contours (Lee & Nguyen, 2001; Peterhans & von der Heydt, 1989; von der Heydt et al., 1984), complex shapes (Hegdé & Van Essen, 2000, 2003, 2004; Mahon & DeValois, 2001), and surface boundaries (Baumann, van der Zwan, & Peterhans, 1997; Zhou et al., 2000). Based on the anatomical connections and physiological properties of neurons of V2, it appears to be a good candidate for study of the early stage of form vision.

We find that a quasi-linear model provides a good account of the responses of V2 neurons to translational Glass patterns presented within their CRF, consistent with our previous findings for V1 neurons (Smith et al., 2002). V2 neurons show surround suppression to grating stimuli that was similar to that found in V1 neurons. We wondered if V2 neurons might show selectivity for concentric or radial Glass pattern form presented outside of their CRF, but we found no evidence for such selectivity. Together, our data suggest that V2 neurons add little to the computation provided by V1 neurons of the global form present in Glass patterns. Our previous results (Smith et al., 2002) show that V1 is capable of providing the fundamental signals necessary for the detection of local structure in Glass patterns. We recorded in V2 to determine how these signals are combined for further processing.

Our first set of experiments was aimed at comparing V2 responses with V1 responses to translational Glass pattern stimuli. We might expect V2 neurons to be more responsive or sharply tuned to these patterns because of the potential for combining inputs from V1 cells. However, responses to gratings are similar in V1 and V2 (Levitt et al., 1994), which might lead us to expect similar Glass pattern responses in V1 and V2. Our data support the latter hypothesis. When using translational Glass pattern stimuli, we found a striking similarity in response properties in the two areas. The orientation tuning preference, optimal dot separation, and modulation in firing rate were largely indistinguishable between V1 and V2. We conclude that for V2 neurons, as for V1 neurons, a quasi-linear model provides a good fit for responses to translational Glass patterns presented within the CRF.

Having found no differences between V1 and V2 in response to translational Glass pattern stimuli presented in the CRF, we then explored whether V2 neurons might integrate information over larger regions of visual space around their CRFs. One major question about the neural processing of form perception is the relative importance of mechanisms that pool information within and outside the CRF of a neuron. While neurons with sensitivity to complex shapes within their CRF have been reported in multiple studies, it is also the case

that surround effects are present in multiple visual areas. It is with this latter possibility in mind that we performed our experiments using the full-screen concentric, radial, and translational Glass patterns. Concentric Glass pattern stimuli elicit a stronger percept of global form—Wilson and Wilkinson (1998) and Wilson et al. (1997) found lower thresholds for detection of concentric Glass patterns in noise, as compared with radial or translational Glass patterns. This leads us to believe that individual neuronal responses to Glass patterns in some visual areas might reflect these psychophysical results.

We designed the concentric and radial Glass pattern stimuli so that they would mimic a preferred translational Glass pattern as closely as possible within the CRF. We might have expected the response to the concentric or radial stimuli to be higher than that to the translational pattern for two reasons. One possibility is that signals related to the global form might be reflected in the responses of these neurons to concentric or radial stimuli, producing a higher response. Alternatively, the extended oriented structure in the full-screen translational pattern might activate iso-oriented surround mechanisms, suppressing the cell's response. We found that responses were broadly similar to the translational, concentric, and radial stimuli. The response to the translational pattern was the highest on average, slightly larger than the response to concentric or radial patterns. Furthermore, among the concentric and radial patterns, there was a systematic variation in response with the center position (more distant center positions produced a larger response). These findings are easily explained by examining how dot-pair orientation changes over space. For concentric and radial patterns, the stimulus was configured to have nearly optimal dot-pair orientation in the CRF. When the stimulus is centered outside the CRF, the orientation of the dot pairs changes away from optimal. This is particularly true for the "near" patterns, where the CRF is closer to the center of rotation or expansion. The smaller response for concentric and radial patterns and the variation in response with center position can be explained by nonoptimal CRF stimulation. Petkov and Westenberg (2003) suggested that cells that exhibit iso-orientation surround suppression play a role in contour detection but not in texture detection. Our results are consistent with this suggestion in that V2 cells showed significant surround suppression (average SI of 0.38) and did not show selectivity to the textural shape present in the global form stimuli. However, even V2 neurons in which we observed little or no surround suppression showed no selectivity to global form. In addition, Petkov and Westenberg used one particular class of stimuli (letters with superimposed band-spectrum noise) in their study. It is unclear how their results generalize to other classes of stimuli. Thus, the role of iso-orientation surround suppression in texture segmentation remains an open question.

Previous work on Glass pattern perception has proposed that significant global integration may first occur at the level of V4 neurons. Wilson and Wilkinson (1998) created a model in which area V4 neurons detected Glass pattern form by pooling the output of a filter–rectify–filter sequence occurring in V1 and V2. In human psychophysical experiments, Cardinal and Kiper (2003) and, later, Mandelli and Kiper (2005) examined the detection of chromatic, circular Glass patterns. Their results are consistent with the idea that analysis of local dot-pair orientation occurs in V1 and V2 neurons, whereas global spatial integration takes place in an area with receptive fields the size of V4 or larger. Our results provide evidence that area V2 plays a role similar to V1 in the processing of the sparse local orientation cues present in Glass pattern stimuli within the CRF. V2 neurons may play an important role in the processing of illusory contours and surface boundaries under some stimulus conditions. However, we found no evidence for sensitivity in V2 neurons to global form information present in Glass pattern stimuli extending outside the CRF. There are several possible reasons for this. First, Glass pattern stimuli may not sufficiently drive circuits that are present in V2 and able to detect global form outside the CRF. Additionally, attention may influence neuronal responses to spatial configuration in the awake animal. Second, neurons

in V2 able to detect global form outside the CRF, but neurons in some higher visual area might. Third, the computation of global form may actually take place within the large CRFs of cells in higher levels of the visual system. Neurons in V4 and IT respond selectively to complex form stimuli presented within their CRF and have significantly larger receptive fields than those found in V1 or V2. A study of their responses to Glass pattern stimuli might help reveal the mechanisms of Glass pattern perception.

Acknowledgments

This work was supported by a research grant from the NIH (NEI EY02017) and by an HHMI Investigatorship to J.A.M. M.A.S. was supported in part by an NEI Institutional Training Grant (T32-7136). We thank Wyeth Bair for helpful advice and discussion.

References

Alliston EL, Friehling MS, Smith MA, Landy MS, Movshon JA. Detectability of global form in Glass patterns and random dot motion stimuli depends only on signal-to-noise ratio. Investigative Ophthalmology & Visual Science 2001;42:4683.

Allman J, Miezin F, McGuinness E. Stimulus specific responses from beyond the classical receptive field: Neurophysiological mechanisms for local–global comparisons in visual neurons. Annual Review of Neuroscience 1985;8:407–430. [PubMed].

Barlow HB, Olshausen BA. Convergent evidence for the visual analysis of optic flow through anisotropic attenuation of high spatial frequencies. Journal of Vision 2004;4(6):415–426. 1, http://journalofvision.org/4/6/1/, doi:10.1167/4.6.1. [PubMed] [Article]. [PubMed: 15330709]

Baumann R, van der Zwan R, Peterhans E. Figure-ground segregation at contours: A neural mechanism in the visual cortex of the alert monkey. European Journal of Neuroscience 1997;9:1290–1303. [PubMed]. [PubMed: 9215713]

Blakemore C, Tobin E. Lateral inhibition between orientation detectors in the cat's visual cortex. Experimental Brain Research 1972;15:439–440. [PubMed].

Born RT. Center-surround interactions in the middle temporal visual area of the owl monkey. Journal of Neurophysiology 2000;84:2658–2669. [PubMed] [Article]. [PubMed: 11068007]

Bradley DC, Andersen RA. Center-surround antagonism based on disparity in primate area MT. Journal of Neuroscience 1998;18:7552–7565. [PubMed] [Article]. [PubMed: 9736673]

Brincat SL, Connor CE. Underlying principles of visual shape selectivity in posterior inferotemporal cortex. Nature Neuroscience 2004;7:880–886. [PubMed].

Cardinal KS, Kiper DC. The detection of colored Glass patterns. Journal of Vision 2003;3(3):199–208. 2, http://journalofvision.org/3/3/2/, doi:10.1167/3.3.2. [PubMed] [Article]. [PubMed: 12723965]

Cavanaugh JR, Bair W, Movshon JA. Nature and interaction of signals from the receptive field center and surround in macaque V1 neurons. Journal of Neurophysiology 2002a;88:2530–2546. [PubMed] [Article]. [PubMed: 12424292]

Cavanaugh JR, Bair W, Movshon JA. Selectivity and spatial distribution of signals from the receptive field surround in macaque V1 neurons. Journal of Neurophysiology 2002b;88:2547–2556. [PubMed] [Article]. [PubMed: 12424293]

Dakin SC. The detection of structure in Glass patterns: Psychophysics and computational models. Vision Research 1997;37:2227–2246. [PubMed]. [PubMed: 9578905]

Dakin SC, Bex PJ. Local and global visual grouping: Tuning for spatial frequency and contrast. Journal of Vision 2001;1(2):99–111. 4, http://journalofvision.org/1/2/4/, doi:10.1167/1.2.4. [PubMed] [Article]. [PubMed: 12678605]

DeAngelis GC, Freeman RD, Ohzawa I. Length and width tuning of neurons in the cat's primary visual cortex. Journal of Neurophysiology 1994;71:347–374. [PubMed]. [PubMed: 8158236]

DeValois KK, Switkes E. Spatial frequency interaction of dot patterns and gratings. Proceedings of the National Academy of Sciences of the United States of America 1980;77:662–665. [PubMed] [Article]. [PubMed: 6928651]

Earle DC. Perception of Glass pattern structure with stereopsis. Perception 1985;14:545–552. [PubMed]. [PubMed: 3836386]

Gallant JL, Braun J, Van Essen DC. Selectivity for polar, hyperbolic, and Cartesian gratings in macaque visual cortex. Science 1993;259:100–103. [PubMed]. [PubMed: 8418487]

Gallant JL, Connor CE, Rakshit S, Lewis JW, Van Essen DC. Neural responses to polar, hyperbolic, and Cartesian gratings in area V4 of the macaque monkey. Journal of Neurophysiology 1996;76:2718–2739. [PubMed]. [PubMed: 8899641]

Glass L. Moire effect from random dots. Nature 1969;223:578–580. [PubMed]. [PubMed: 5799528]

Glass L, Perez R. Perception of random dot interference patterns. Nature 1973;246:360–362. [PubMed]. [PubMed: 4586322]

Glass L, Switkes E. Pattern recognition in humans: Correlations which cannot be perceived. Perception 1976;5:67–72. [PubMed]. [PubMed: 958850]

Hegdé J, Van Essen DC. Selectivity for complex shapes in primate visual area V2. Journal of Neuroscience 2000;20:RC61. [PubMed] [Article]. [PubMed: 10684908]

Hegdé J, Van Essen DC. Strategies of shape representation in macaque visual area V2. Visual Neuroscience 2003;20:313–328. [PubMed]. [PubMed: 14570253]

Hegdé J, Van Essen DC. Temporal dynamics of shape analysis in macaque visual area V2. Journal of Neurophysiology 2004;92:3030–3042. [PubMed] [Article]. [PubMed: 15201315]

Hubel D, Wiesel T. Receptive fields and functional architecture of monkey striate cortex. Journal of Physiology 1968;195:215–243. [PubMed] [Article]. [PubMed: 4966457]

Knierim JJ, Van Essen DC. Neuronal responses to static texture patterns in area V1 of the alert macaque monkey. Journal of Neurophysiology 1992;67:961–980. [PubMed]. [PubMed: 1588394]

Kobatake E, Tanaka K. Neuronal selectivities to complex object features in the ventral visual pathway of the macaque cerebral cortex. Journal of Neurophysiology 1994;71:856–867. [PubMed]. [PubMed: 8201425]

Lamme VAF. The neurophysiology of figure-ground segregation in primary visual cortex. Journal of Neuroscience 1995;15:1605–1615. [PubMed]. [PubMed: 7869121]

Lee TS, Nguyen M. Dynamics of subjective contour formation in early visual cortex. Proceedings of the National Academy of Sciences of the United States of America 2001;98:1907–1911. [PubMed] [Article]. [PubMed: 11172049]

Lee TS, Yang CF, Romero RD, Mumford D. Neural activity in early visual cortex reflects behavioral experience and higher-order perceptual saliency. Nature Neuroscience 2002;5:589–597. [PubMed].

Leventhal AG, Thompson KG, Lui D, Zhou Y, Ault SJ. Concomitant sensitivity to orientation, direction, and color of cells in layers 2, 3, and 4 of monkey striate cortex. Journal of Neuroscience 1995;15:1808–1818. [PubMed] [Article]. [PubMed: 7891136]

Levitt JB, Kiper DC, Movshon JA. Receptive fields and functional architecture of macaque V2. Journal of Neurophysiology 1994;71:2517–2542. [PubMed]. [PubMed: 7931532]

Mahon LE, DeValois RL. Cartesian and non-Cartesian responses in LGN, V1, and V2 cells. Visual Neuroscience 2001;18:973–981. [PubMed]. [PubMed: 12020088]

Mandelli MJ, Kiper DC. The local and global processing of chromatic Glass patterns. Journal of Vision 2005;5(5):405–416. 2, http://journalofvision.org/5/5/2/, doi:10.1167/5.5.2. [PubMed] [Article]. [PubMed: 16097872]

Movshon JA, Smith MA, Kohn A. Responses to glass patterns in macaque V1 and V2 [Abstract]. Journal of Vision 2003;3(9):151. 151a http://journalofvision.org/3/9/151/, doi:10.1167/3.9.151.

Movshon JA, Thompson ID, Tolhurst DJ. Spatial summation in the receptive fields of simple cells in the cat's striate cortex. Journal of Physiology 1978;283:53–77. [PubMed] [Article]. [PubMed: 722589]

Nelson JI, Frost BJ. Orientation-selective inhibition from beyond the classical visual receptive field. Brain Research 1978;139:359–365. [PubMed]. [PubMed: 624064]

Nothdurft HC, Gallant JL, Van Essen DC. Response modulation by texture surround in primate area V1: Correlates of "popout" under anesthesia. Visual Neuroscience 1999;16:15–34. [PubMed]. [PubMed: 10022475]

Nothdurft HC, Gallant JL, Van Essen DC. Response profiles to texture border patterns in area V1. Visual Neuroscience 2000;17:421–436. [PubMed]. [PubMed: 10910109]

O'Keefe LP, Movshon JA. Processing of first- and second-order motion signals by neurons in area MT of the macaque monkey. Visual Neuroscience 1998;15:305–317. [PubMed]. [PubMed: 9605531]

Pasupathy A, Connor CE. Responses to contour features in macaque area V4. Journal of Neurophysiology 1999;82:2490–2502. [PubMed] [Article]. [PubMed: 10561421]

Pasupathy A, Connor CE. Shape representation in area V4: Position-specific tuning for boundary conformation. Journal of Neurophysiology 2001;86:2505–2519. [PubMed] [Article]. [PubMed: 11698538]

Pasupathy A, Connor CE. Population coding of shape in area V4. Nature Neuroscience 2002;5:1332–1338. [PubMed].

Peterhans E, von der Heydt R. Mechanisms of contour perception in monkey visual cortex: II. Contours bridging gaps. The Journal of Neuroscience 1989;9:1749–1763. [PubMed] [Article]. [PubMed: 2723748]

Peterhans E, von der Heydt R. Functional organization of area V2 in the alert macaque. European Journal of Neuroscience 1993;5:509–524. [PubMed]. [PubMed: 8261126]

Petkov N, Westenberg MA. Suppression of contour perception by band-limited noise and its relation to nonclassical receptive field inhibition. Biological Cybernetics 2003;88:236–246. [PubMed]. [PubMed: 12647231]

Prazdny K. On the perception of Glass patterns. Perception 1984;13:469–478. [PubMed]. [PubMed: 6527934]

Prazdny K. Some new phenomena in the perception of Glass patterns. Biological Cybernetics 1986;53:153–158. [PubMed]. [PubMed: 3947684]

Ross J, Badcock D, Hayes A. Coherent global motion in the absence of coherent velocity signals. Current Biology 2000;10:679–682. [PubMed] [Article]. [PubMed: 10837253]

Sceniak MP, Ringach DL, Hawken MJ, Shapley R. Contrast's effect on spatial summation by macaque V1 neurons. Nature Neuroscience 1999;2:733–739. [PubMed].

Schein SJ, Desimone R. Spectral properties of V4 neurons in the macaque. The Journal of Neuroscience 1990;10:3369–3389. [PubMed] [Article]. [PubMed: 2213146]

Skottun BC, DeValois RL, Grosof DH, Movshon JA, Albrecht DG, Bonds AB. Classifying simple and complex cells on the basis of response modulation. Vision Research 1991;31:1079–1086. [PubMed]. [PubMed: 1909826]

Smith MA, Bair W, Movshon JA. Signals in macaque V1 neurons that support the perception of Glass patterns. Journal of Neuroscience 2002;22:8334–8345. [PubMed] [Article]. [PubMed: 12223588]

Solomon SG, Peirce JW, Lennie P. The impact of suppressive surrounds on chromatic properties of cortical neurons. Journal of Neuroscience 2004;24:148–160. [PubMed] [Article]. [PubMed: 14715948]

Thomas OM, Cumming BG, Parker AJ. A specialization for relative disparity in V2. Nature Neuroscience 2002;5:472–478. [PubMed].

von der Heydt R, Peterhans E, Baumgartner G. Illusory contours and cortical neuron responses. Science 1984;224:1260–1262. [PubMed]. [PubMed: 6539501]

Wilson HR, Wilkinson F. Detection of global structure in Glass patterns: Implications for form vision. Vision Research 1998;38:2933–2947. [PubMed]. [PubMed: 9797989]

Wilson HR, Wilkinson F, Asaad W. Concentric orientation summation in human form vision. Vision Research 1997;37:2325–2330. [PubMed]. [PubMed: 9381668]

Zhou H, Friedman HS, von der Heydt R. Coding of border ownership in monkey visual cortex. Journal of Neuroscience 2000;20:6594–6611. [PubMed] [Article]. [PubMed: 10964965]

Zipser K, Lamme VA, Schiller PH. Contextual modulation in primary visual cortex. Journal of Neuroscience 1996;16:7376–7389. [PubMed] [Article]. [PubMed: 8929444]

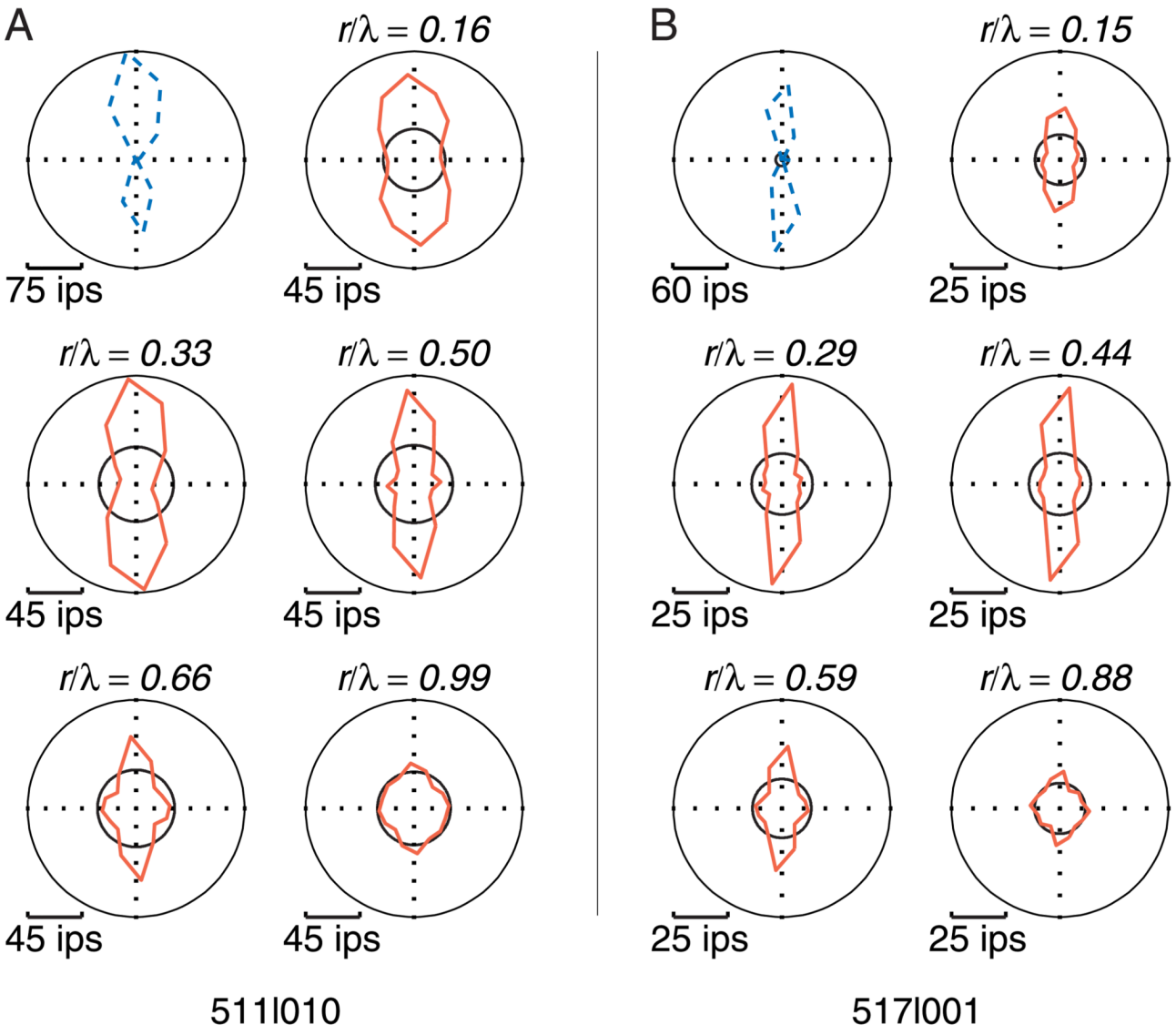

Figure 1.

Sample responses of two V2 neurons. (A and B) The left and right panels of this figure show the responses of two V2 neurons to gratings and Glass patterns. The direction tuning for drifting sinusoidal gratings is shown in the polar plot in the upper left of each panel with a *blue dotted line*. Translational Glass pattern tuning curves taken at multiple dot separations (*r*) are shown in the remaining plots with *red solid lines*. The values of *r*/λ are indicated at the top of each polar plot. The black circles on each polar plot represent baseline responses, consisting of a blank gray screen for gratings and random dots for Glass patterns. The Glass pattern polar plots are presented with a different scale than the grating to better show their features.

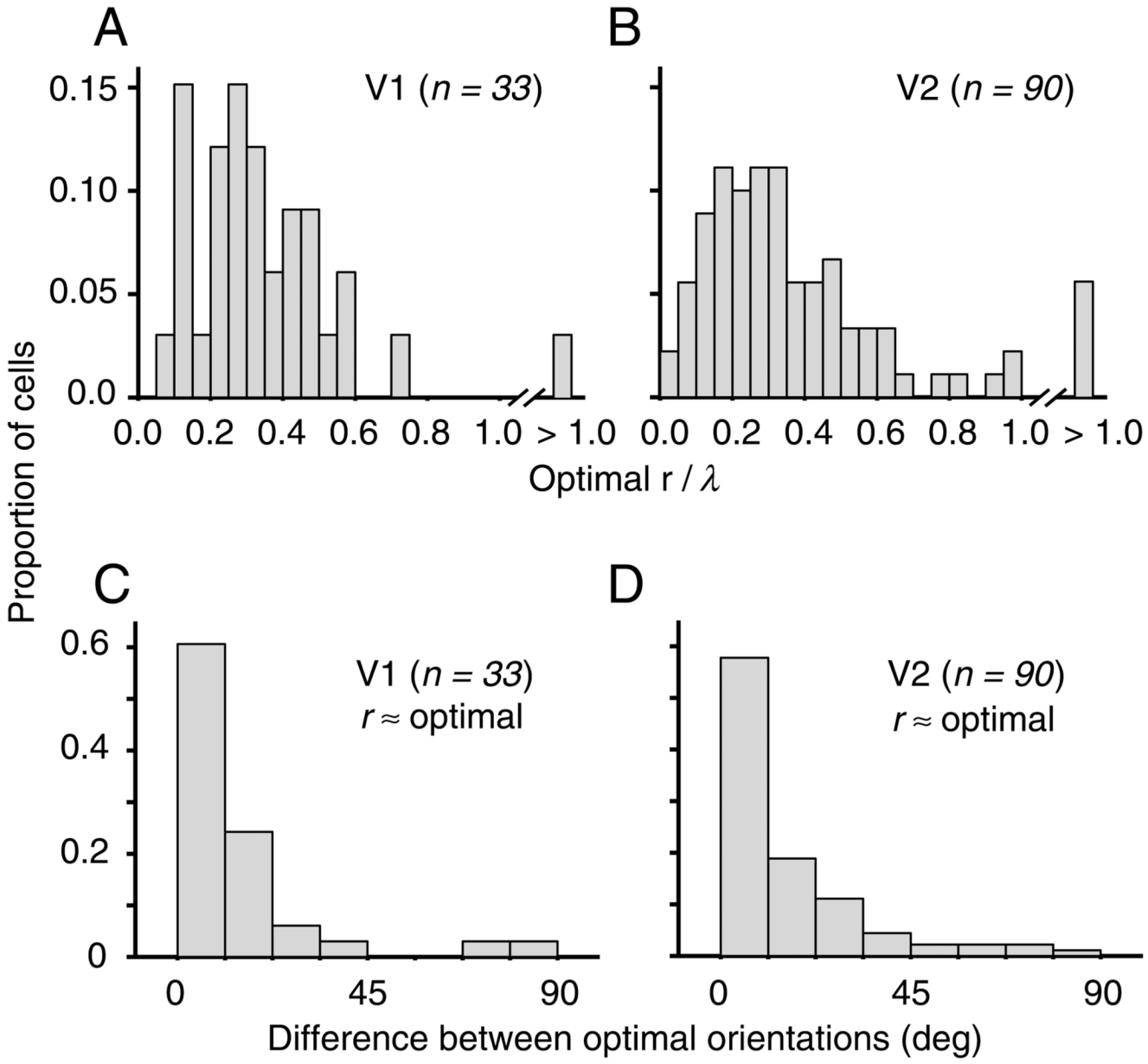

Figure 2.

Orientation tuning and dot separation in V1 and V2. (A) The frequency histogram of r/λ values associated with the maximal selectivity in the Glass pattern tuning curves in V1 shows that selectivity was highest for most cells (94%) when dot separation was less than 0.6 of the optimal spatial frequency. (B) The comparable frequency histogram of r/λ values in V2 shows that selectivity was highest for most cells (84%) in the same range as V1, when dot separation was less than 0.6 of the optimal spatial frequency. (C) The frequency histogram of the absolute value of the difference between the preferred grating orientation and the preferred Glass pattern orientation at $r/\lambda < 0.6$ has a prominent peak near 0°. Thus, Glass pattern tuning in V1 was similar when measured with traditional or continuous-sequence stimuli (compare with data from Smith et al., 2002). Simple and complex cells had similar distributions and are combined here. (D) In V2, the trend shown is identical to that

shown in Panel C. (E) We performed the same analysis for preferred Glass pattern orientation when r/λ was between 0.7 and 1.3 in V1. In this case, the tuning for gratings and Glass patterns also tends to be aligned. The alignment is not as strong as when $r/\lambda < 0.6$. (F) The results in V2 are again similar to V1 (see Panel E).

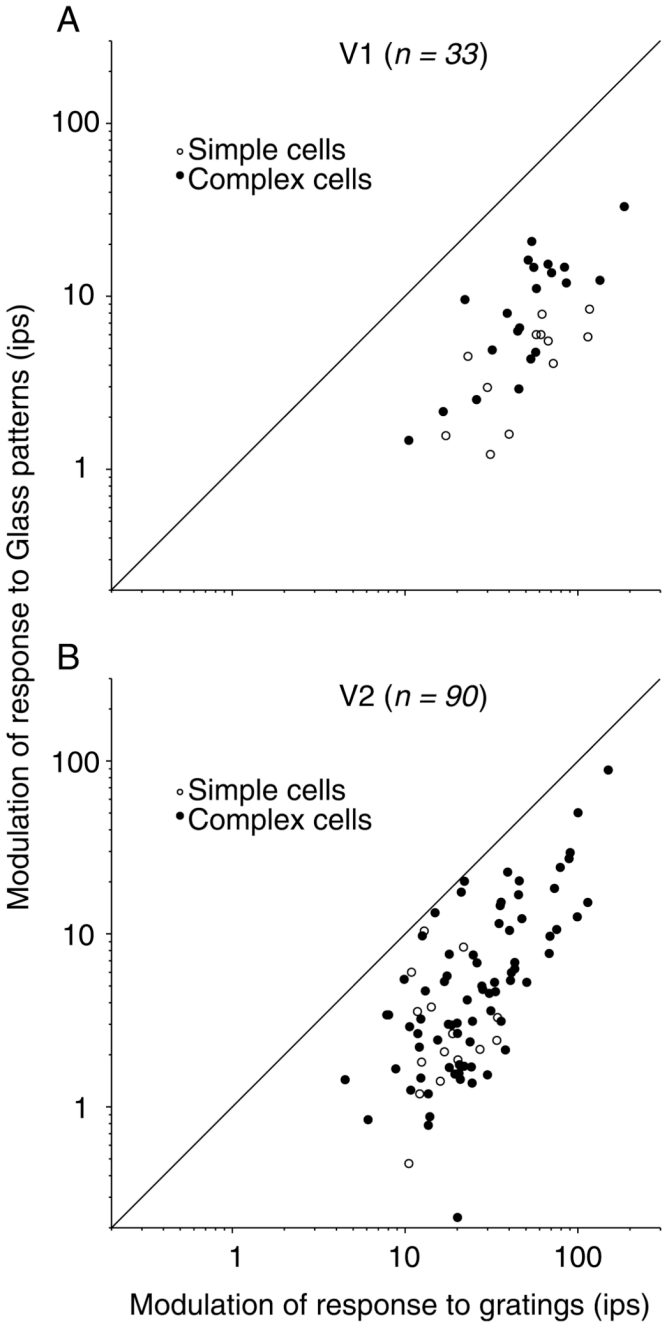

Figure 3.

Responses to Glass patterns and gratings in V1 and V2. (A) For each cell, we defined the response modulation to be the maximum response minus the minimum response (or the peak minus the trough of the orientation tuning curve). For Glass patterns, we used the tuning curve taken at the optimal dot separation. Responses are plotted for both complex cells (filled circles) and simple cells (open circles) in V1. All points fall below the diagonal line of equality, indicating that all cells responded better, that is, had more modulated tuning curves, to gratings than to Glass patterns. (B) In V2, the trend shown is similar to that shown in Panel A.

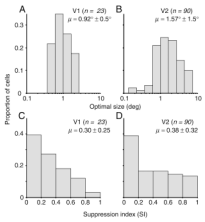

Figure 4.

Optimal size and surround suppression for gratings in V1 and V2. (A) We recorded the response to gratings of increasing size and fit the resulting tuning curve (see the Methods section). For this analysis, we only included the 23 V1 neurons recorded on the operculum, whose eccentricity matched that of the recorded V2 neurons. In this group, at a mean eccentricity of 3.0° (ranging from 2.1° to 4.1°), the geometric mean diameter was 0.92°. This is similar to that reported by Cavanaugh et al. (2002a; our “optimal size” is calculated in the same way as their GSF diameter metric) for V1 neurons in a similar eccentricity range. (B) In V2, at a mean eccentricity of 3.8° (ranging from 1.8° to 6.3°), receptive fields appear roughly 1.5 times as large (in diameter) as V1 receptive fields. (C) We calculated an SI, the peak response minus the response at the maximum size, divided by the response at the maximum size. It ranges from 0 (for no suppression) to 1 (for complete suppression). The average value of this index for our data (0.30) is close to that found previously for V1 neurons (Cavanaugh et al., 2002a; Smith et al., 2002). (D) For V2 neurons, we found an SI (0.38) similar to the value from our population of V1 neurons.

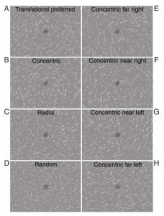

Figure 5.

Glass pattern stimuli used to test for global form sensitivity in V2 neurons. (A–D) After finding the optimal θ and *r*, we tested neurons with Glass patterns that filled our video display (12.9° × 9.3°). The overlaid receptive field indicates the position, orientation, and size of the recorded neuron. We used the four types of patterns shown—translational (A), concentric (B), radial (C), and random (D). The translational pattern was shown at either a preferred or an orthogonal orientation. The concentric and radial patterns were shown with four center positions, position along a line perpendicular or parallel to the preferred orientation of the cell, respectively. This made the dots that fall within the CRF similar to those in the translational pattern. (E–H) These panels show the four center positions that were used in the concentric Glass pattern. There are two positions, one near and one far, on each side of the CRF center (Movie 2).

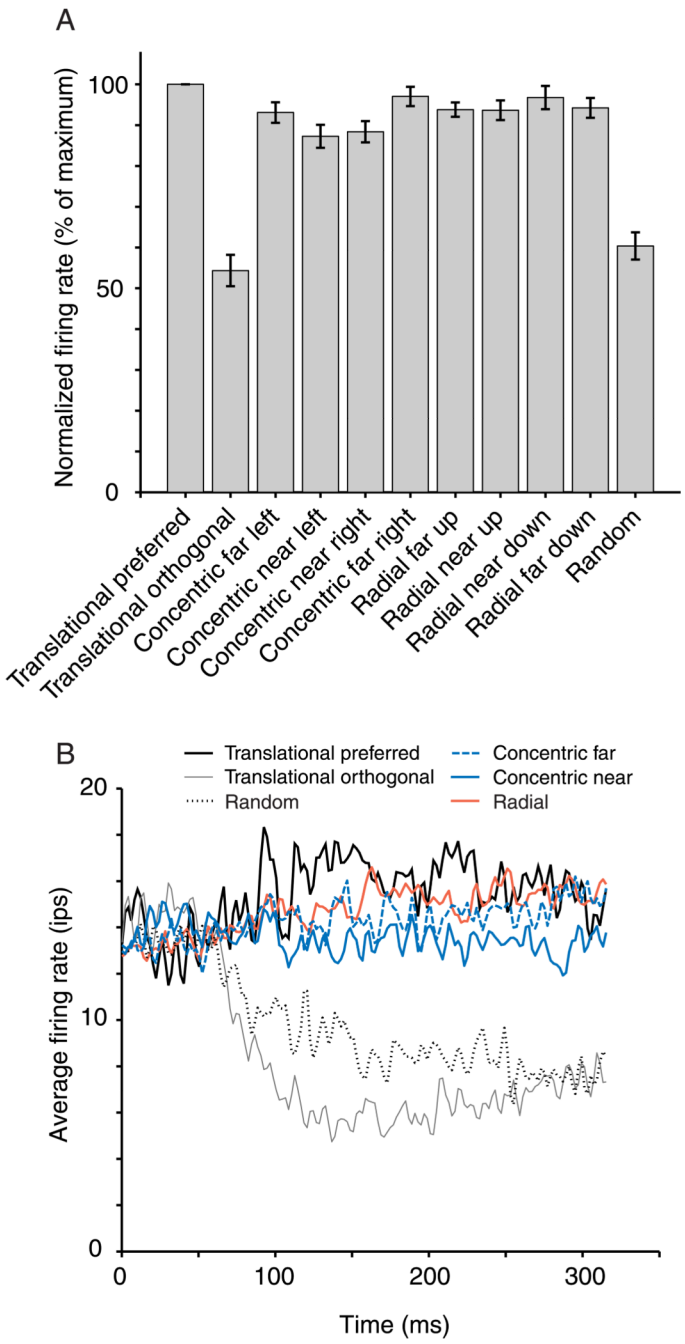

Figure 6.

Normalized responses of V2 neurons to Glass pattern stimuli. (A) For 20 neurons, we took the response of each neuron to the 11 stimuli and divided it by that cell's response to the preferred translational pattern. These normalized responses for all cells were averaged together (error bars represent ±1 *SEM*). Responses to the preferred translation pattern were the highest, and responses to the orthogonal pattern were the lowest. We presented the concentric and radial stimuli centered on four positions each (two on each side of the CRF center, aligned so that the dot pairs in the CRF would be near optimal in orientation). They are labeled "near" and "far" for Positions A and B. These patterns evoked responses (though slightly lower) that were similar to the preferred translational pattern. (B) We averaged the

responses of 20 neurons to create a mean PSTH for each stimulus. At approximately 60 ms after the stimulus transition (Time 0), the response curves for the different stimuli diverge. It is notable that the average response prior to this time is quite high, about 14 ips. This is due to the stimulus history, in which 9 of the 11 stimuli evoked a reasonably strong response, whereas only two (orthogonal and random) caused a reduced response. On average, the best response throughout the stimulation period is to the preferred translational pattern. The concentric and radial patterns, which are averaged across the four positions each, evoke a response that is slightly smaller.

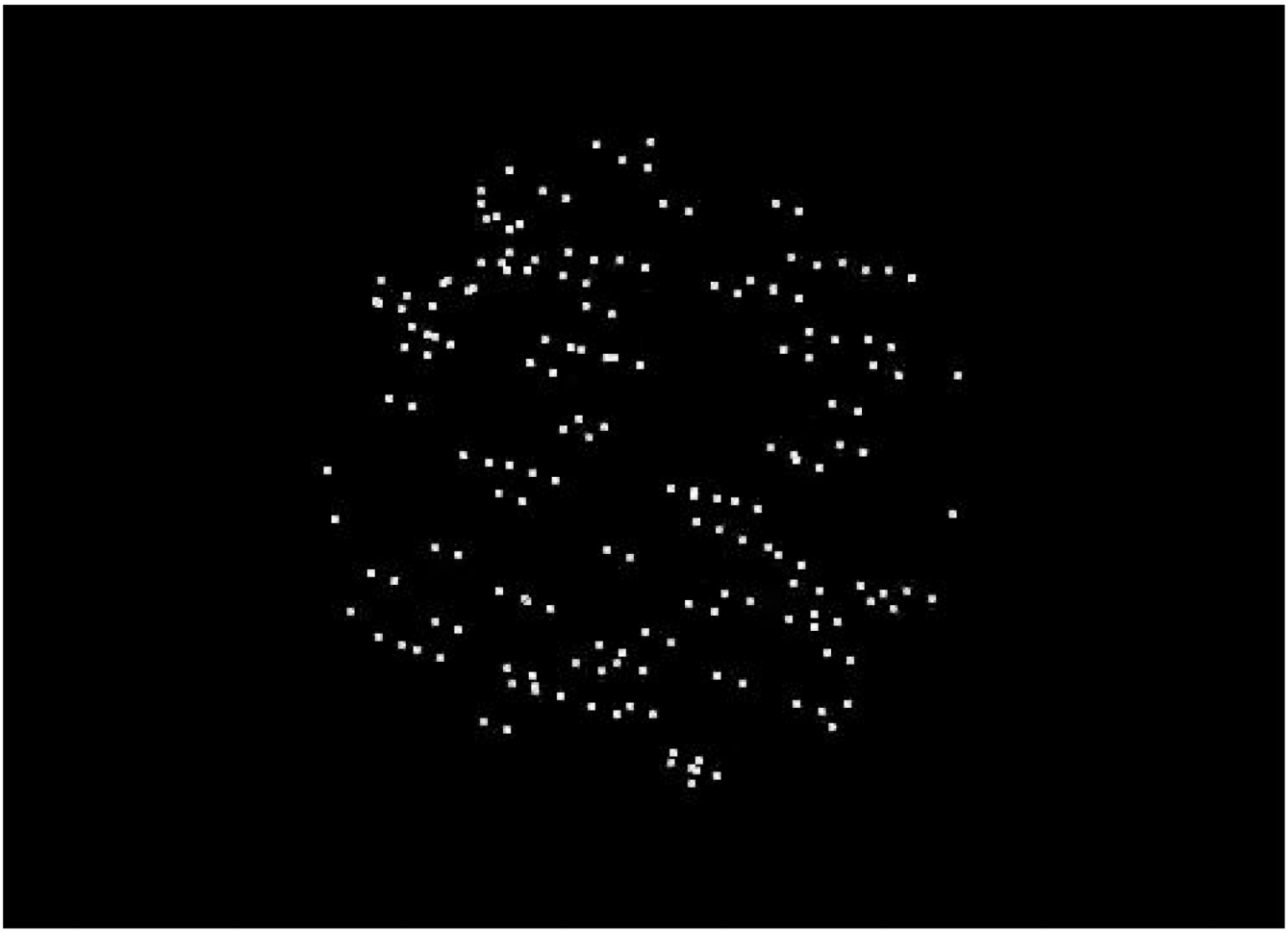

Movie 1.
Translational Glass pattern stimulus. Click on the image to view the movie.

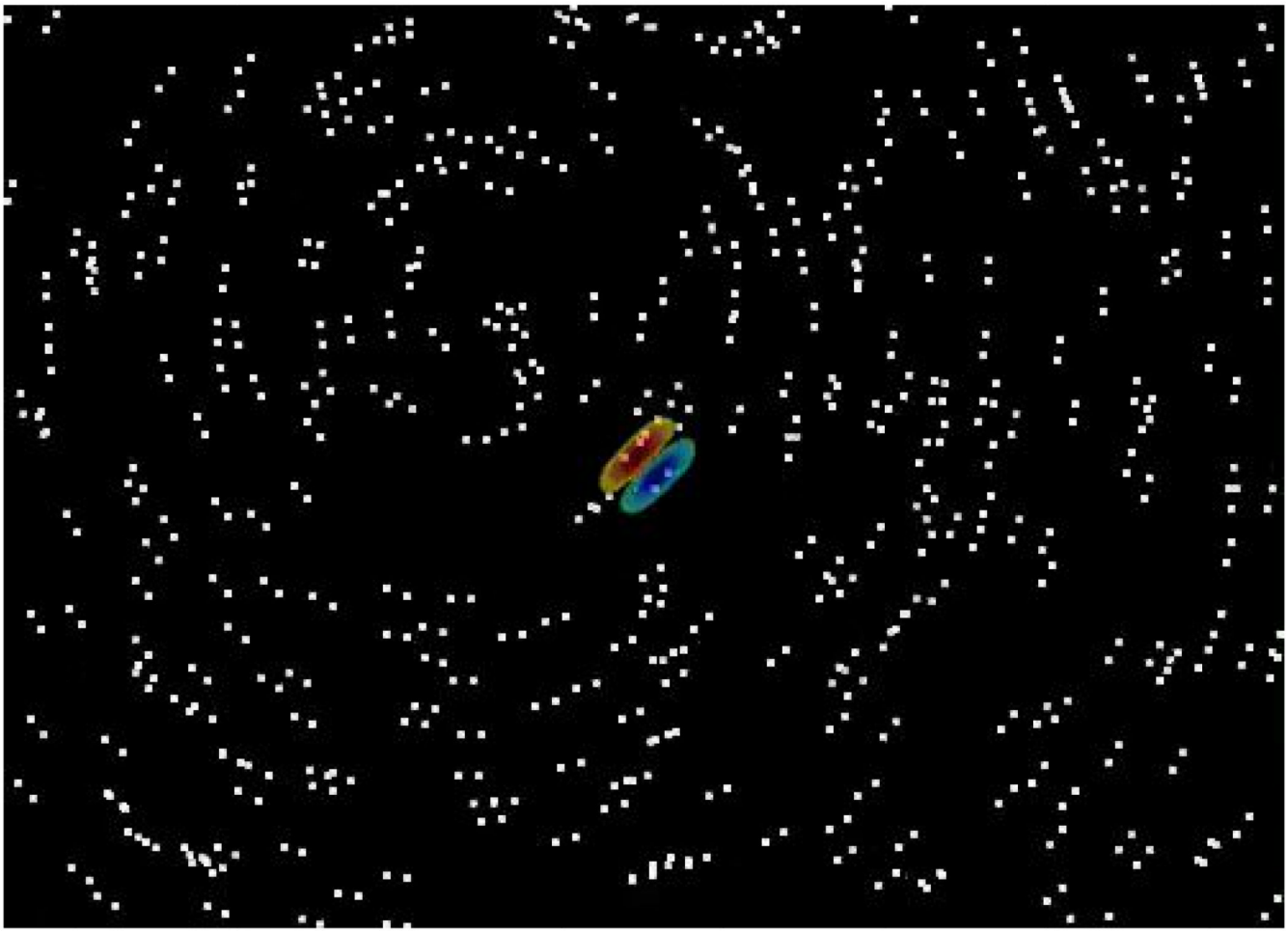

Movie 2.
Glass pattern global form stimulus. Click on the image to view the movie.

Table 1

Selectivity of orientation tuning for Glass patterns in V2. This table contains an analysis of V2 data, which are comparable to those from Smith et al. (2002) for V1. We calculated an orientation and quadropole selectivity index (see the Methods section) for Glass pattern orientation tuning when $r \approx \lambda/2$ and $r \approx \lambda$, the mean of which is shown in the four entries on the left side of the table. The fraction of cells for which the selectivity index was statistically significant (see the Methods section) is shown in the four entries on the right side of the table. We used a Wilcoxon test to assess the significance of the differences in selectivity index on the left and a χ^2 homogeneity test for differences in the fraction of cells on the right. For each pair of table entries, the probability value for the appropriate statistic is shown in italics below or to the right of the pair of numbers being compared. Both of the measures show that two-lobed tuning dominates when $r \approx \lambda/2$. When $r \approx \lambda$, the four-lobed tuning may be present, but the data do not appear to be as strong as those shown for V1 in the study of Smith et al. For comparison, the mean orientation selectivity index for gratings was 0.58, with 87 of 90 tuning curves significantly selective.

	Selectivity index			Fraction significant		
r	**Orientation**	**Quadropole**	**Significance**	**Orientation**	**Quadropole**	**Significance**
λ/2	0.56	0.27	*.0001*	69/90	15/90	*.0001*
λ	0.36	0.34	*.4185*	17/58	14/58	*.675*
Significance	*.0001*	*.0013*		*.0001*	*.365*	

Table 2

Firing rates of V1 and V2 neurons to Glass pattern and gratings. For each cell, the response modulation for Glass patterns and gratings was calculated as the peak minus the trough of the orientation tuning curve. Glass pattern tuning curves were taken at the optimal dot separation. The data in this table show the geometric mean of this response modulation for simple and complex cells in V1 and V2. We also present the V1 data from Smith et al. (2002) for comparison. In addition, we present the geometric mean of the response ratio (of grating to Glass pattern) for both simple and complex cells in V1 and V2. The numbers of cells for each group are shown in parenthesis after this ratio. The response ratio was consistently higher in simple cells (than in complex cells) and in V1 cells (than in V2 cells).

	Complex		Simple	
	Grating	**Glass pattern**	**Grating**	**Glass pattern**
V1	48.7	7.8	49.4	3.9
	Ratio = 6.2 (n = 21)		Ratio = 12.6 (n = 12)	
V2	25.8	4.8	16.9	2.6
	Ratio = 5.4 (n = 75)		Ratio = 6.5 (n = 15)	